CALCULATION OF CRACK WIDTHS WITH THE σ–ε METHOD

David Dupont and Lucie Vandewalle
Katholieke Universiteit Leuven, Belgium.

Abstract
Durability of concrete is in a great extent determined by the crack widths that are formed in the structure and that allow water to infiltrate in the concrete so that corrosion of the reinforcement bars can occur. This paper concerns the calculation of crack widths in beams containing longitudinal reinforcement and steel fibres. Two calculation methods are explained. The first is the calculation method that is proposed by Rilem TC162-TDF. This method is a semi-empirical method, based on the approach followed by Eurocode 2 for normal concrete. The second method is a more fundamental approach that considers the interaction between the concrete and the reinforcement bars. Both calculation methods have been compared with experimental results of 19 full-scale beams. The investigated parameters were the reinforcement ratio, the fibre content, the fibre type and the shear span to depth ratio. The comparison between experimental and theoretical results shows that for both models a relatively good prediction can be found of the average crack width.

1. Introduction

The determination of cracks in concrete has always been a topic of interest for investigation by many scientists. In general it is assumed that the durability of the structure is assured when the crack widths are limited to 0.3 mm. One of the often-used approaches to limit the crack widths is the use of steel fibre reinforced concrete (SFRC). Steel fibre concrete is generally known to reduce crack widths because of its post-cracking tensile strength.

At the Department of Civil Engineering of the Catholic University of Leuven, Belgium, a test program has been executed on 19 full-scale SFRC beams containing longitudinal reinforcement. All beams have been tested in four-point bending. The tests were performed in different load steps until failure of the beam. The load steps were chosen so that the beams failed after 10 to 15 steps. At each load step the crack widths and spacings were measured. The results of the test program illustrate the strong beneficial effect of steel fibres on the crack width as well as on the crack spacing. The addition of fibres to the concrete can lead to a reduction of the crack width of up to 40%.

The crack widths of the beams of the test program have also been calculated by means of the calculation method proposed by Rilem TC162-TDF [1] as well as with a newly developed physical cracking model for reinforced SFRC beams. The model takes into account the bond between the reinforcement bars and the SFRC matrix as well as the influence of the steel fibres. A comparison

of the calculated results and the experimental results shows that there is a relatively good correlation between the two.

2. Calculation methods

2.1 Calculation method proposed by Rilem TC162-TDF [1].

In the most recent recommendation of Rilem TC162-TDF the calculation of crack widths is done with a semi-empirical method, which is based on the method used in Eurocode 2 for the calculation of crack widths in concrete without steel fibres. The mean crack width w_m may be calculated by:

$$w_m = \varepsilon_{sm} \cdot s_{rm} \tag{1}$$

with : s_{rm} = the average final crack spacing (mm);
ε_{sm} = the mean steel strain allowed under the relevant combination of loads for the effects of tension stiffening, shrinkage, etc.

The average final crack spacing for members subjected principally to flexure or normal force can be calculated from the equation:

$$s_{rm} = \left(50 + 0.25\, k_1\, k_2 \frac{\phi_b}{\rho_r}\right)\left(\frac{50}{L_f/\phi_f}\right) \tag{2}$$

with : $\dfrac{50}{L_f/\phi_f} \le 1$

ϕ_b = the bar size in mm;
k_1 = a coefficient which takes account of the bond properties of the bars;
k_2 = a coefficient which takes account of the form of the strain distribution;
ρ_r = the effective reinforcement ratio $A_s/A_{c,eff}$ where A_s is the area of reinforcement contained within the effective tension area $A_{c,eff}$;
L_f = the fibre length in mm;
ϕ_f = the fibre diameter in mm.

The mean steel strain ε_{sm} is obtained from the relation:

$$\varepsilon_{sm} = \frac{\sigma_s}{E_s}\left(1 - \beta_1\, \beta_2 \left(\frac{\sigma_{sr}}{\sigma_s}\right)^2\right) \tag{3}$$

with : σ_s = the stress in the tensile reinforcement calculated on the basis of a cracked section as shown in a (MPa);
σ_{sr} = the stress in the tensile reinforcement calculated on the basis of a cracked section under loading conditions causing first cracking as presented in Figure 1a (MPa);
β_1 = a coefficient which takes account of the bond properties of the bar [2];
β_2 = a coefficient which takes account of the duration of the load or of repeated loading [2];
E_s = Young's modulus for steel reinforcement (MPa).

Figure 1: Assumed stress distribution for plain concrete (a) and SFRC (b) beam section.

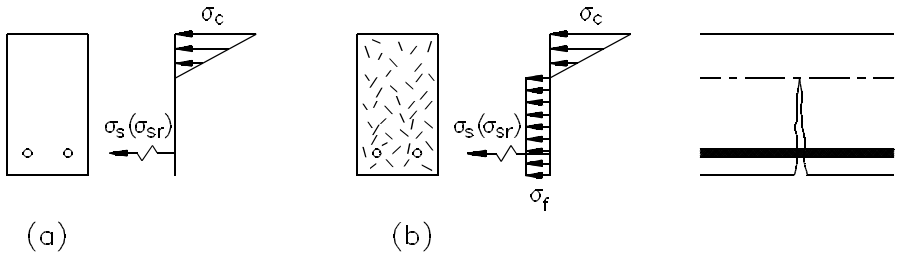

In the calculation the fibres have an implicit influence on ε_{sm}, because the fibres reduce the steel stresses σ_s and σ_{sr}. The stress σ_f (b) is taken equal to 0.45 $f_{R,1}$ [1], where $f_{R,1}$ is determined by means of a bending test on a notched prism according to the new RILEM proposal [1]. The beneficial influence of the fibres on the mean final crack spacing is found in the last factor of equation (2).

2.2 Alternative calculation method

The Rilem proposal is a rather easy method that is very close to the approach in Eurocode 2 [2]. However, the method is an empirical method. In search for a more fundamental calculation method, the authors have developed a new physical model. In Figure 2, a fragment of a beam is shown. Section 2 is a cracked section, while section 1 is a section that is just about to crack. The length L of the fragment is the minimum crack spacing for a given moment M. The maximum crack spacing is equal to 2L. It is concluded from this that the average crack spacing is equal to $1.5 \cdot L$. The general calculation procedure consists of two steps. In a first step the length L in Figure 2 is determined, assuming that the tensile stress in section 1 is equal to 1.2 times the tensile strength f_{ctm} and that the tensile stength in section 2 is equal to 0.8 times f_{ctm}. The factors 1.2 and 0.8 are introduced to take the scatter on the tensile strength of the concrete into account. In the second step, the length of the beam fragment is fixed at $0.75 \cdot L$ (half of the average crack spacing) and now the tensile stress in section 1 is variable.

Figure 2: Beam part between a cracked section and a section that has just reached the point of cracking.

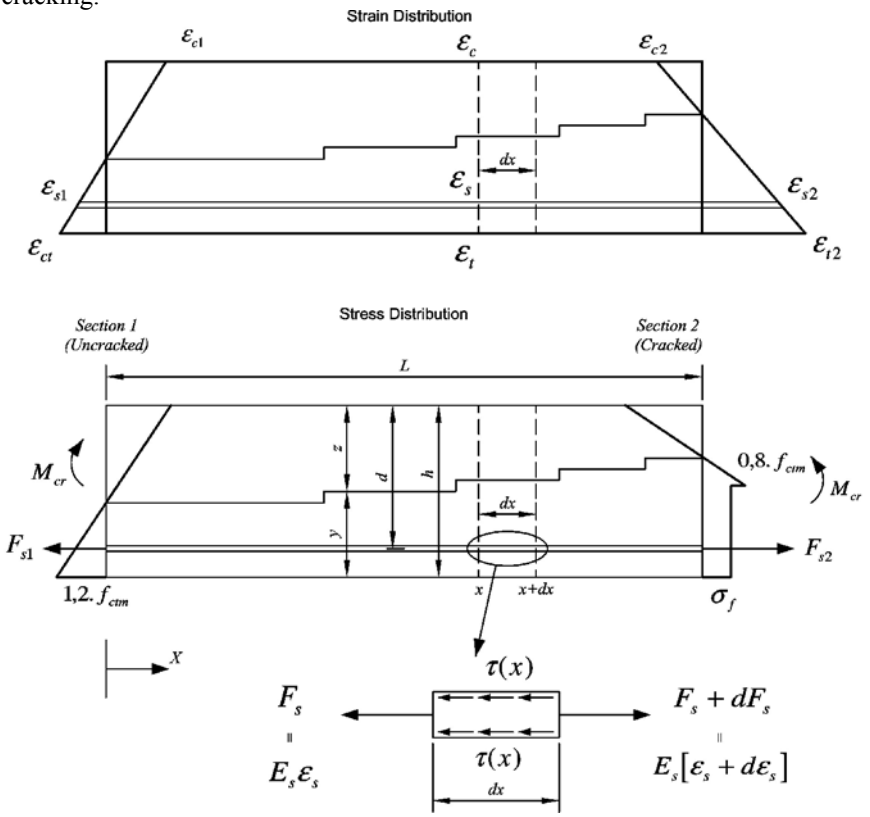

It is assumed that the influence of the fibres in section 2 can be simulated wit a drop-constant stress-strain relation. The drop-constant relation is considered to be a special case of the two-level model [4]. The stress σ_f is calculated as $0.39 \cdot f_{R,1}$. The stress-strain relation for the post-cracking behaviour of SFRC implies that there is a full co-operation between the SFRC and the reinforcement bar. The stress-strain relation was determined assuming a perfectly linear strain distribution over the entire cross section. In reality however, this is not the case. In a cracked section and in the immediate neighbourhood, the reinforcement bars slip in the concrete matrix. The slip δ is maximal at the place of cracking and zero at a place that is far enough away from the crack. In a section where a new crack is formed, the slip is also assumed to be zero. This is because on both sides of the future crack the slip is opposite. In this calculation model the slip is assumed to be zero in section 1. Section 1 is an uncracked section.

For the calculation of the crack spacing it is assumed that the position of the neutral axis can be calculated exactly in section 1 and section 2 by using static equilibria of axial forces and bending moments in these sections. For all sections that lie in between section 1 and 2, the position of the neutral axis is unknown. It is assumed here that position of the neutral axis is constant over a small interval and can be calculated as follows:

$$z_x = z_1 + \frac{z_2 - z_1}{\delta_2}\delta_x \tag{4}$$

where: z_x, z_1 and z_2 are the positions of the neutral axis in section x, section 1 and section 2, respectively; δ_2 is the slip in section 2 and δ_x is the slip in a section x. To start the calculations a value of δ_2 must be assumed and afterwards, if this slip was not correct, an iteration step can be performed.

In step one the unknown parameters are:
-) the length L;
-) the steel strain in section 1: ε_{s1};
-) the steel strain in section 2: ε_{s2};
-) the compressive strain in section 1: ε_{c1};
-) the compressive strain in section 2: ε_{c2};
-) the concrete tensile strain in section 2: ε_{t2};
-) the position of the neutral axis: y and z;
-) the slip δ as function of x.

For the calculation of the length L and the slip δ, a differential equation must be solved. All other unknown parameters can be solved by simple static equilibrium of forces and moments. According to the hypothesis of Bernouilli, the following relations can be written:

$$\varepsilon_s = \varepsilon_t \frac{d-z}{y} \tag{5}$$

$$\varepsilon_c = \varepsilon_t \frac{z}{y} \tag{6}$$

Requiring static equilibrium of normal forces for section 1 results in:

$$\frac{1}{2} b\, z\, E_c\, \varepsilon_{c1} = \frac{1}{2} b\, y\, E_c \varepsilon_{t1} + A_s E_s \varepsilon_{s1} - A_s E_c \varepsilon_{t1} \frac{d-z}{y} \tag{7}$$

Requiring static equilibrium of normal forces in section 2 results in:

$$\frac{1}{2} b\, z\, E_c \varepsilon_{c2} = \frac{1}{2} b\, y\, f_{ct} \frac{\varepsilon_{ct}}{\varepsilon_{t2}} + b\, y\, \sigma_f \left(1 - \frac{\varepsilon_{ct}}{\varepsilon_{t2}}\right) + A_s\, E_s\, \varepsilon_{s2} - A_s\, \sigma_f \tag{8}$$

Requiring static equilibrium of moments for section 1 results in:

$$\frac{1}{3} b\, z^2 E_c \varepsilon_{c1} + \frac{1}{3} b y^2 E_c \varepsilon_{t1} + A_s E_s \varepsilon_{s1} (d-z) - A_s E_c \varepsilon_{t1} \frac{(d-z)^2}{y} = M \tag{9}$$

Requiring static equilibrium of moments for section 2 results in:

$$\frac{1}{3} b\, z^2 E_c \varepsilon_{c2} + \frac{1}{3} b\, y^2\, f_{ct} \left(\frac{\varepsilon_{ct}}{\varepsilon_{t2}}\right)^2 + \left(b\, y\, \sigma_f \left(1 - \frac{\varepsilon_{ct}}{\varepsilon_{t2}}\right)\right)\left(\frac{y \varepsilon_{ct}}{2\varepsilon_{t2}} + \frac{y}{2}\right) + \left(A_s\, E_s\, \varepsilon_{s2} - A_s\, \sigma_f\right)(d-z) = M \tag{10}$$

From equations (8) and (10) the strain ε_{t2} and the position of the neutral axis y can be found. Following this, from equations (7) and (9) the strains ε_{s1} and ε_{c1} can be found. This results in the complete knowledge of stresses and strains in sections 1 and 2. The only remaining unknown parameters are the length L and the slip δ as a function of x. If a static equilibrium of normal

forces and moments is written for an arbitrary section at place x, equations (11) and (12) are found:

$$\frac{1}{2} b\, z\, E_c \varepsilon_c = \frac{1}{2} b\, y\, E_c \varepsilon_t + A_s \left(E_s \varepsilon_s - E_c \varepsilon_t \frac{d-z}{y} \right) \tag{11}$$

$$\frac{1}{3} b\, z^2 E_c \varepsilon_c + A_s \left(E_s \varepsilon_s - E_c \varepsilon_t \frac{d-z}{y} \right)(d-z) + \frac{1}{3} b\, y^2 E_c \varepsilon_t = M \tag{12}$$

Extracting ε_c from equation (11) gives:

$$\varepsilon_c = \frac{y}{z} \varepsilon_t + \frac{2A_s}{b\, z\, E_c} \left(E_s \varepsilon_s - E_c \varepsilon_t \frac{d-z}{y} \right) \tag{13}$$

Substituting equation (13) into equation (12) gives:

$$\begin{aligned} &\frac{1}{3} b\, z^2 E_c \left[\frac{y}{z} \varepsilon_t + \frac{2A_s}{b\, z\, E_c} \left(E_s \varepsilon_s - E_c \varepsilon_t \frac{d-z}{y} \right) \right] \\ &+ A_s \left(E_s \varepsilon_s - E_c \varepsilon_t \frac{d-z}{y} \right)(d-z) + \frac{1}{3} b\, y^2 E_c \varepsilon_t = M \end{aligned} \tag{14}$$

From equation (14), ε_t can be written as a function of ε_s:

$$\varepsilon_t = \frac{M - A_s E_s \varepsilon_s \left(d - \frac{z}{3} \right)}{\frac{1}{3} b\, y\, h\, E_c - A_s E_c \frac{d-z}{y} \left(d - \frac{z}{3} \right)} \tag{15}$$

This leaves only the strain ε_s to be determined. The position of the neutral axis (y and z) in any section is assumed to be the same as in section 2. Since the steel rebars are slipping relative to the surrounding concrete, the steel strain is composed of two parts. The first part is the strain of the surrounding concrete, while the second part is the strain due to the slipping of the rebars:

$$\varepsilon_s = \varepsilon_t \frac{d-z}{y} + \frac{d\delta(x)}{dx} \tag{16}$$

Equation (15) is substituted in equation (16):

$$\frac{d\delta(x)}{dx} = \varepsilon_s - \frac{M - A_s E_s \varepsilon_s \left(d - \frac{z}{3} \right)}{\frac{1}{3} b\, y\, h\, E_c - A_s E_c \frac{d-z}{y} \left(d - \frac{z}{3} \right)} \cdot \frac{d-z}{y} \tag{17}$$

If the derivative of equation (17) is calculated, then equation (18) is found. It is assumed here that the moment M is independent of the position x along the longitudinal axis, i.e. the bending moment is constant in this zone of the beam.

$$\frac{d^2\delta(x)}{dx^2} = \frac{d\varepsilon_s}{dx}\left[1 + \frac{A_s E_s\left(d - \frac{z}{3}\right)(d-z)}{\frac{1}{3} b\, y^2 h\, E_c - A_s E_c (d-z)\left(d - \frac{z}{3}\right)}\right] \tag{18}$$

To solve this differential equation a relation must be found between the slip δ and the strain ε_s, both functions of x. The horizontal equilibrium of the steel reinforcement between the place x and the place x + dx results in (Figure 2):

$$\underbrace{A_s E_s \varepsilon_s + \tau(x)\cdot\pi\cdot\Sigma\phi\cdot dx = A_s E_s(\varepsilon_s + d\varepsilon_s)}_{\frac{d\varepsilon_s}{dx} = \tau(x)\frac{\pi\cdot\Sigma\phi}{E_s A_s}} \tag{19}$$

Substituting expression (19) in equation (18) results in:

$$\frac{d^2\delta(x)}{dx^2} = \tau(x)\underbrace{\frac{\pi\cdot\Sigma\phi}{E_s A_s}\left[1 + \frac{A_s E_s\left(d - \frac{z}{3}\right)(d-z)}{\frac{1}{3} b\, y^2 h\, E_c - A_s E_c (d-z)\left(d - \frac{z}{3}\right)}\right]}_{A} \tag{20}$$

Now only a relation has to be assumed describing $\tau(x)$ as a function of $\delta(x)$. This chosen τ–δ relation is equation (21).

$$\tau = \tau_{max}\left(1 - \mu\, e^{-\lambda\delta}\right) \tag{21}$$

The determination of τ_{max} is explained in [4, 5, 6]. Recent research at the department of Civil Engineering of the Catholic University of Leuven has shown that μ and λ can be determined from pullout tests. μ as well as λ are dependent on the concrete cover. The addition of steel fibers has only an influence on μ. The reason is that μ is to a great extent determined by the chemical bond between reinforcement bar and surrounding concrete. If fibers are added to the concrete this has a negative impact on the degree of compaction. For the concrete cover used in this test program it was found that λ can be taken equal to 8, while μ can be taken equal to 0.782 for plain concrete and equal to 0.89 for SFRC with 60 kg/m^3 fibers of type RC 65/60 BN. For other fiber dosages an interpollation is used. Substituting equation (21) in equation (20) gives:

$$\frac{d^2\delta(x)}{dx^2} = A\,\tau_{max}\left(1 - \mu\, e^{-\lambda\delta(x)}\right) \tag{22}$$

To solve equation (22), a few new parameters are introduced:

$$\lambda\cdot\delta(x) = \varphi(x) \qquad \underbrace{\sqrt{\tau_{max}\cdot A\cdot\lambda}}_{a}\cdot x = \alpha \qquad p = \frac{d\varphi}{d\alpha} = \varphi' \tag{23}$$

Equation (22) can now be written as:

$$\underbrace{\varphi'' = \frac{d\,p}{d\alpha} = \frac{d\,p}{d\varphi}\frac{d\varphi}{d\alpha} = \frac{d\,p}{d\varphi}p = \varphi'\frac{d\varphi'}{d\varphi}}$$
$$\Downarrow$$
$$\varphi'\frac{d\varphi'}{d\varphi} = 1-\mu\, e^{-\varphi}$$
$$\Downarrow$$
$$\varphi'\,d\varphi = \left(1-\mu\, e^{-\varphi}\right)d\varphi \tag{24}$$

If this last expression is integrated, equation (25) is obtained:

$$\varphi'^2 = 2\cdot\int\left(1-\mu\, e^{-\varphi}\right)d\varphi$$
$$\Downarrow$$
$$\varphi'^2 = 2\left[\varphi+\mu\cdot e^{-\varphi}\right]+C_1 \tag{25}$$

For the determination of the integration constant C_1 the following boundary conditions have been taken into account:

$$\text{For}\quad x=0\rightarrow\begin{cases}\delta = 0 \quad\Rightarrow\quad \varphi = 0\\ \dfrac{d\delta}{dx} = \varepsilon_{s1}-\varepsilon_{t1}\dfrac{d-z}{y} \quad\Rightarrow\quad \varphi' = \dfrac{\lambda\cdot\varepsilon_{s1}}{a}-\dfrac{\lambda}{a}\varepsilon_{t1}\dfrac{d-z}{y}\end{cases} \tag{26}$$

In case the beam is loaded with the cracing moment, which we assume for the calculation of the crack spacing, the second boundary condition is equal to 0. This results in:

$$C_1 = \left[\frac{\lambda\varepsilon_{s1}}{a}-\frac{\lambda\varepsilon_{t1}}{a}\left(\frac{d-z}{y}\right)\right]^2-2\mu \tag{27}$$

Equation (25) can now be used to determine the course of the slip δ as function of x:

$$\varphi' = \frac{d\varphi}{d\alpha} = \sqrt{2\left(\varphi+\mu\, e^{-\varphi}\right)+\left[\frac{\lambda\varepsilon_{s1}}{a}-\frac{\lambda\varepsilon_{t1}}{a}\left(\frac{d-z}{y}\right)\right]^2-2\mu}$$
$$\Downarrow$$
$$\int_0^{\alpha}d\alpha = \int_0^{\varphi}\frac{d\varphi}{\sqrt{2\left(\varphi+\mu\, e^{-\varphi}\right)+\left[\frac{\lambda\varepsilon_{s1}}{a}-\frac{\lambda\varepsilon_{t1}}{a}\left(\frac{d-z}{y}\right)\right]^2-2\mu}} \tag{28}$$

Integrating expression (28) leads to:

$$\alpha+C_2 = ax+C_2 = \underbrace{\int\frac{d\varphi}{\sqrt{2\left(\varphi+\mu\, e^{-\varphi}\right)+\left[\frac{\lambda\varepsilon_{s1}}{a}-\frac{\lambda\varepsilon_{t1}}{a}\left(\frac{d-z}{y}\right)\right]^2-2\mu}}}_{F} \tag{29}$$

The integration constant C_2 in equation (29) is determined with the following boundary condition:

$$x = 0 \quad \rightarrow \quad \begin{cases} \alpha = 0 \\ \delta = 0 \end{cases} \quad \Rightarrow \quad \varphi = 0 \tag{30}$$

Equation (29) cannot be solved analytically. Therefore a numerical procedure has been worked out. At first the integration constant C_2 is determined. This constant is linked to the starting value of the integration interval. If the integration is started at the point 0, then C_2 can be found by substituting $\varphi = 0$ in F (the function after the integration sign). Furthermore the determination of the slip δ as function of x is done by means of an inverse procedure. First the function F is determined for a list of values of φ, starting with zero. After that a numerical integration can be performed and point after point for each value of φ, a corresponding x can be found. Once the course of φ or δ is known as a function of x, the length L can be calculated. This is done by considering the difference in force in the steel reinforcement. This difference must be equal to the total shear force between the reinforcement bar and the concrete.

$$\Delta F_s = A_s E_s \left(\varepsilon_{s2} - \varepsilon_{s1}\right) = \pi \cdot \Sigma\phi \cdot \int_0^L \tau(x)dx \tag{31}$$

Following the above explained approach the length L can be determined for a series of different moments, each moment resulting in a different strain distribution in section 1 and 2 and also a different ΔF_s and therefore a different L. The crack spacing is assumed to be equal to $1.5 \cdot L$ [7].

Figure 3: Beam part between a cracked section and a section that lies in between two cracks.

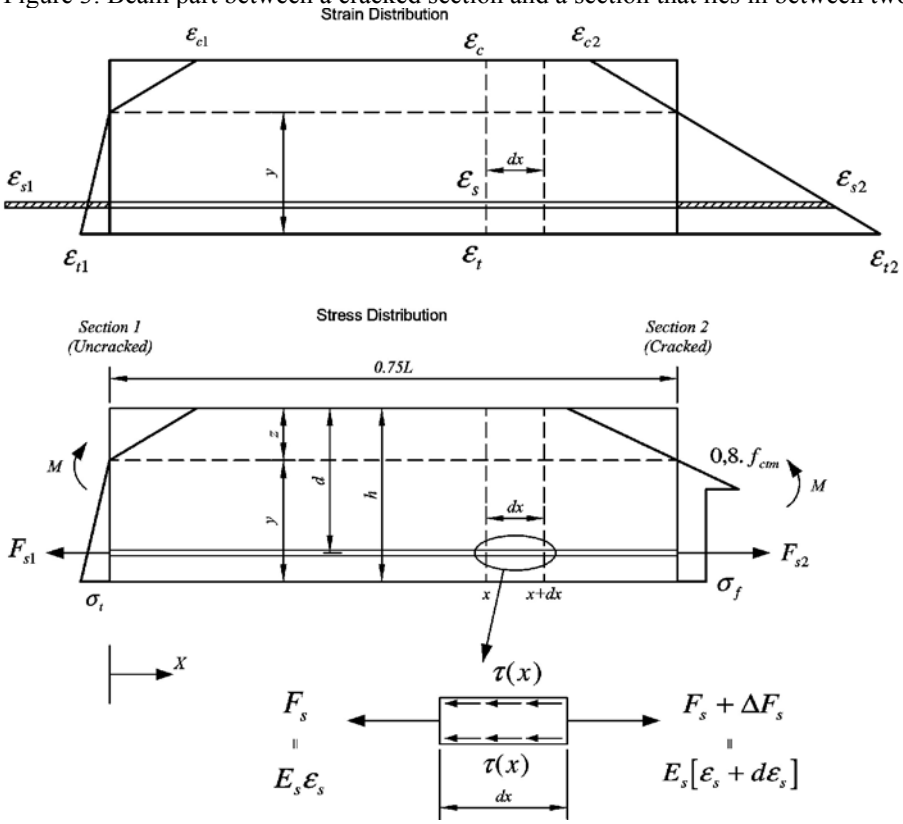

In the second step of the calculation, the crack widths are calculated. Therefore the length of the model is now fixed at half the crack spacing or 0.75L. In section 2 the boundary conditions remain the same, but in section 1, the strain distribution is now different. When the beam is loaded with bending moments that are larger than the cracking moment, the position of the neutral axis shifts upwards. It is therefore assumed here that in step two, where the crack widths are calculated for a certain moment, the position of the neutral axis is fixed and equal to the positionof the neutral axis in the cracked section (Fig. 3). Furthermore, since the length of the model is no longer L, the stress in the bottom fibre of section 1 is now lower than the tensile strength. This means that the strain distribution in section 1 is unknown. To have a system that is in a state of static equilibrium the strain ε_{s1} must be determined so that at a distance x = 0.75L the strain is equal to ε_{s2}. First the steel stress ε_s is calculated as function of x. This can be done by the following steps:

1) From equation (25) and (26) the following relation can be derived:

$$\left[\frac{\lambda\varepsilon_s}{a} - \frac{\lambda\varepsilon_t(d-z)}{a\,y}\right]^2 = 2\left[\varphi + \mu\, e^{-\varphi}\right] + \left[\frac{\lambda\varepsilon_{s1}}{a} - \frac{\lambda\varepsilon_{t1}(d-z)}{a\,y}\right]^2 - 2\,\mu \qquad (32)$$

2) If equation (15) is filled into equation (32), an expression is found for the strain ε_s as function of x:

$$\varepsilon_s = \frac{\sqrt{2\left[\varphi + \mu\, e^{-\varphi}\right] + \left[\frac{\lambda\varepsilon_{s1}}{a} - \frac{\lambda\varepsilon_{t1}(d-z)}{a\,y}\right]^2} - 2\mu \cdot \left[\frac{b\,h\,y\,E_c}{3} - A_s E_c\left(\frac{d-z}{y}\right)\left(d-\frac{z}{3}\right)\right]}{\frac{\lambda}{a}\left[\frac{b\,h\,y\,E_c}{3} + A_s\left(E_s - E_c\right)\left(\frac{d-z}{y}\right)\left(d-\frac{z}{3}\right)\right]} + \frac{(d-z)\cdot M}{y\cdot\left[\frac{b\,h\,y\,E_c}{3} - A_s E_c\left(\frac{d-z}{y}\right)\left(d-\frac{z}{3}\right)\right] + (d-z)A_s E_s\left(d-\frac{z}{3}\right)} \tag{33}$$

Using equation (33), the correct value of ε_{s1} can be found. This is done with an iterative procedure. The strain ε_{s1} is chosen. For this chosen value of ε_{s1} the value of ε_{t1} is determined by requiring static equilibrium in section 1. With this new strain distribution in section 1, equation (29) can be solved numerically. If this equation is solved, the value of φ can be determined that corresponds to x = 0.75L. Substituting this value in equation (33), the new strain $\varepsilon_{s2,new}$ is found. This new strain $\varepsilon_{s2,new}$ must be equal to the strain $\varepsilon_{s2,old}$ that was determined from equations (8) and (10). The procedure is repeated, each time for a new ε_{s1}, until the demand ($\varepsilon_{s2,new} = \varepsilon_{s2,old}$) is satisfied. Once this has been done the average crack width is found as twice the value of the slip δ at a distance x = 0.75 L.

3. Experimental program

At the Department of Civil Engineering of the Catholic University of Leuven (Belgium) a test program was executed which involved four-point bending tests on 19 full-scale beams. All beams had a depth of 300 mm and a width of 200 mm. The span was always equal to 2300 mm. The investigated parameters for the 19 beams were the reinforcement ratio, the fibre dosage and the fibre type. The concrete cover on the longitudinal reinforcement is equal to 30 mm. Details for all beams can be found in Table 1.

Figure 4: Test set-up for all beams.

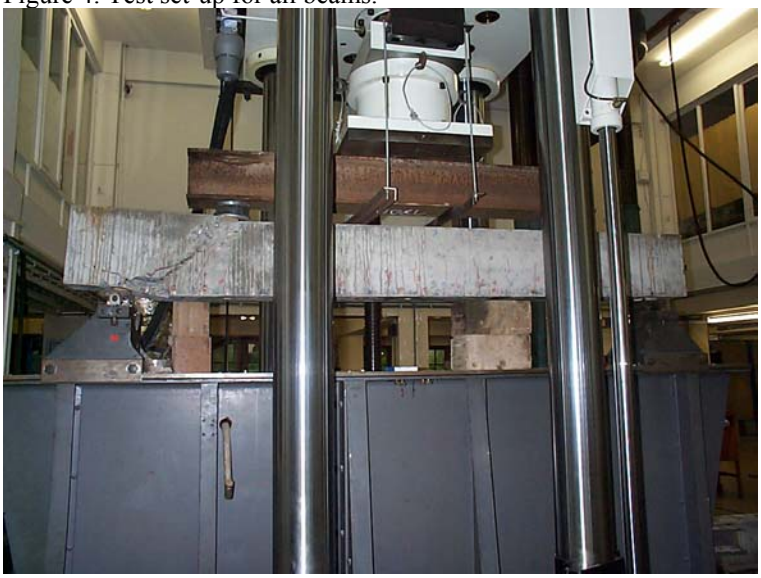

A picture of the test set-up is shown in Figure 4. All beams were tested under load control. The size of the load steps was so that the beam failed after 10 to 15 load step. After each load step the deflection was measured as well as the crack widths on both sides of the beam. The crack widths were measured at ± 1 cm above the bottom of the beam, only in the zone of constant moment (between the loading points). The measurement of the crack widths was done with a small, calibrated microscope. The smallest scale division in the microscope corresponds to 0.02 mm. Furthermore, due to the freaky shapes of the cracks it was sometimes difficult to decide how large the crack width was. Finally it must be said that a crack width can only be measured after the crack has been detected. The smallest crack widths that could be detected had already a crack width of 0.02 to 0.03 mm. This implies that the cracks that have a crack width smaller than 0.02 to 0.03 mm are not detected and not taken into account in the calculation of the average crack width. The result is that the average experimentally observed crack width is a little overestimated. The effect of this becomes more important for beams with a high reinforcement ratio and a high fibre dosage, since for these beams the number of very small cracks that remain undetected is higher. For all these reasons the authors think that, although the measurements were taken with great care, there is a high degree of uncertainty regarding the test results.

Table 1: Test parameters.

Beam	Fibre dosage kg/m^3	Fibre type	Span mm	Reinforcement # x ϕ (mm)
1	0	-	1000	3 ϕ 20
2	20	RC 65/60 BN (*)	1000	3 ϕ 20
3	60	RC 65/60 BN	1000	3 ϕ 20
4	0	-	1000	3 ϕ 16
5	20	RC 65/60 BN	1000	3 ϕ 16
6	60	RC 65/60 BN	1000	3 ϕ 16
7	0	-	1000	3 ϕ 16
8	20	RL 45/50 BN	1000	3 ϕ 16
9	60	RL 45/50 BN	1000	3 ϕ 16
10	0	-	1000	3 ϕ 20
11	20	RL 45/50 BN	1000	3 ϕ 20
12	60	RL 45/50 BN	1000	3 ϕ 20
13	40	RC 65/60 BN	1000	3 ϕ 16
14	40	RC 80/35 BN	1000	3 ϕ 16
15	60	RC 80/35 BN	1000	3 ϕ 16
16	40	RC 65/60 BN	1000	3 ϕ 20
17	0	-	1500	3 ϕ 20
18	20	RC 65/60 BN	1500	3 ϕ 20
19	60	RC 65/60 BN	1500	3 ϕ 20

(*):R : hooked end fibre - C : fibres are glued in bundles - 65 : aspect ratio of fibre (=length/diameter = L/ϕ) - 60 : length of fibre (= L in mm) - B : no coating - N : low carbon, i.e. minimum yield strength of 1100 MPa.

Together with each beam 10 cubes were cast to measure the mean cube compressive strength $f_{cm,cube}$ as well as 8 Rilem 3-point bending specimens to measure the post-cracking behaviour [8]. The mean cylinder compressive strength f_{cm} is taken equal to $0.8 \cdot f_{cm,cube}$. The Young's modulus of steel is taken equal to 200000 MPa, while the Youngs modulus of concrete is calculated with the formula provided in Eurocode 2 [2]:

$$E_c = 9500 \cdot \sqrt[3]{f_c} \ . \tag{35}$$

The tensile strength f_{ctm} is calculated from the flexural strength by applying the size factor proposed by Rilem TC162-TDF [1]:

$$f_{ctm} = f_{ctm,fl} \cdot \frac{1600 - d}{1475} \tag{36}$$

The material properties for all beams are shown in Table 2.

Table 2: Material properties for all beams

Beam	f_{cm} N/mm^2	f_{ctm} N/mm^2	$f_{R,1}$ N/mm^2	$f_{R,4}$ N/mm^2
1	40.2	3.6	0	0
2	40.0	3.5	1.6	1.1
3	38.7	3.9	4.2	3.5
4	40.2	3.6	0	0
5	40.0	3.5	1.6	1.1
6	38.7	3.9	4.2	3.5
7	29.8	3.4	0	0
8	26.8	3.2	1.1	0.8
9	27.5	2.8	2.7	2.1
10	29.8	3.4	0	0
11	26.8	3.2	1.1	0.8
12	27.5	2.8	2.7	2.1
13	48.0	4.7	4.1	3.7
14	46.0	4.5	4.9	2.9
15	50.6	5.0	6.1	3.8
16	47.4	4.4	4.0	3.5
17	40.0	3.5	0	0
18	41.2	4.2	2.3	1.5
19	40.3	4.6	5.9	4.7

The experimental results as well as the theoretical results calculated with the new Rilem method and with the newly developed physical model are shown in Figure 5 until Figure 23.

Figure 5: Experimental and theoretical crack widths for beam 1

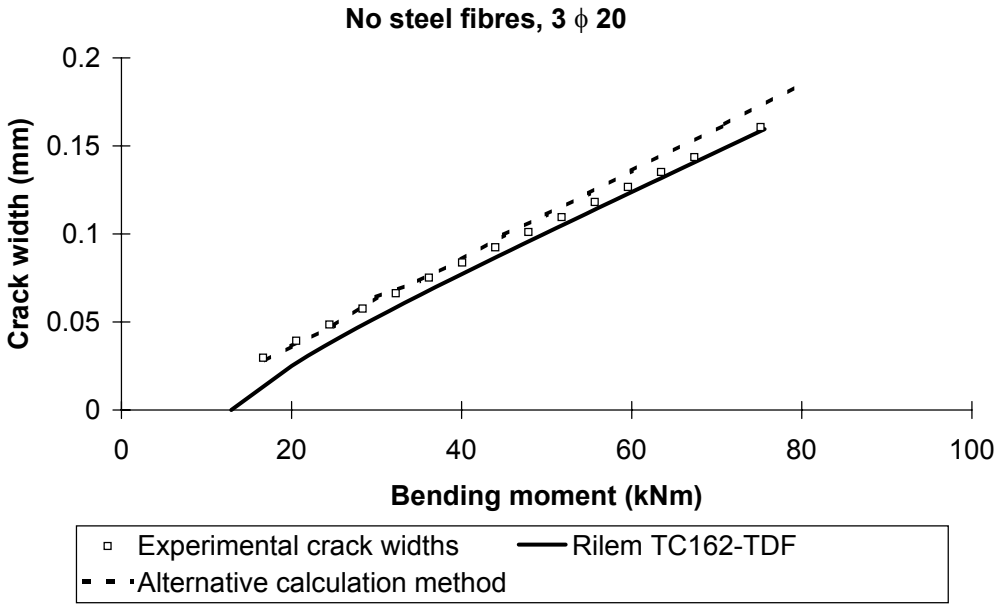

Figure 6: Experimental and theoretical crack widths for beam 2

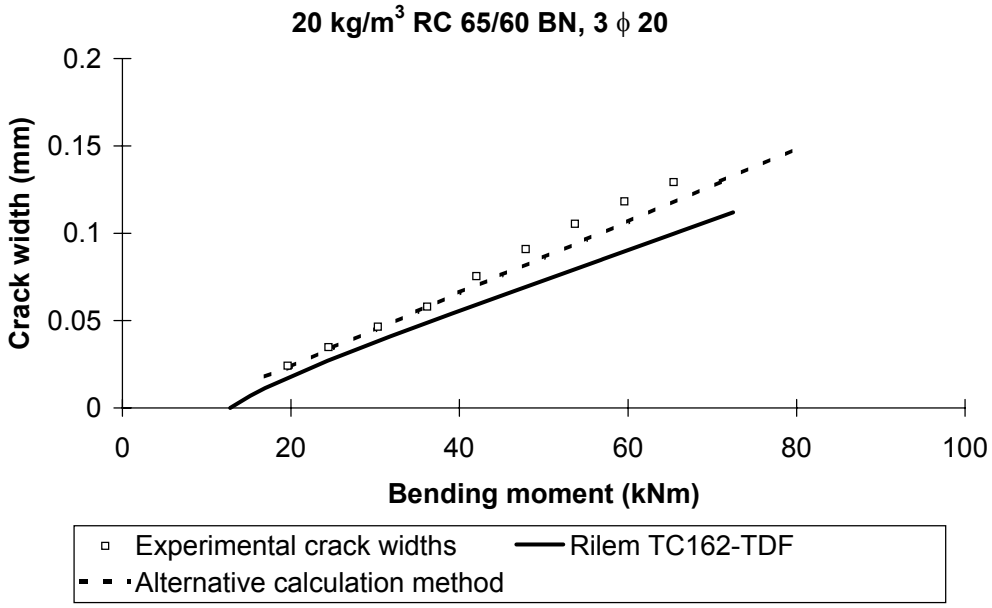

Figure 7: Experimental and theoretical crack widths for beam 3

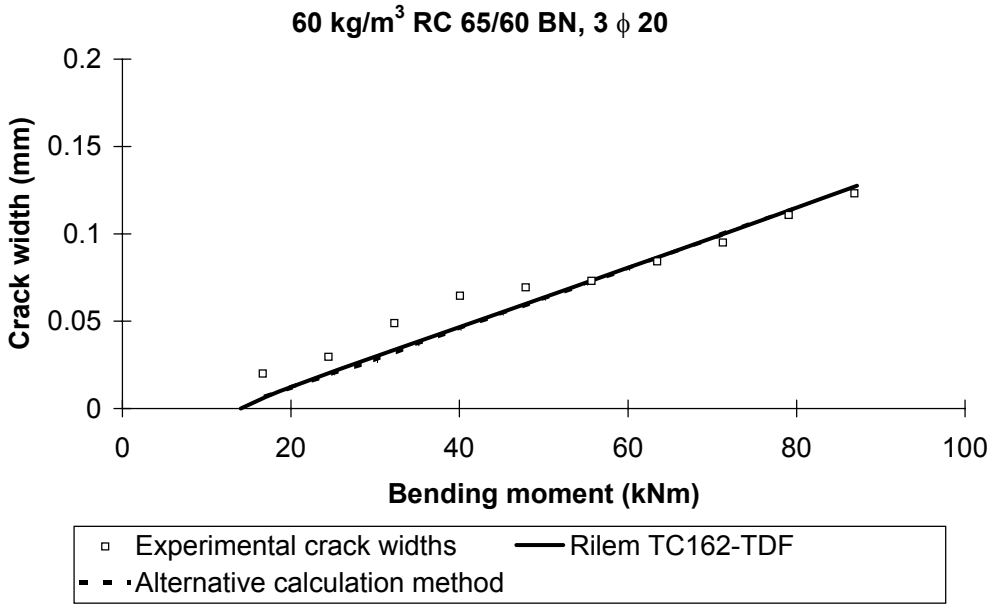

Figure 8: Experimental and theoretical crack widths for beam 4

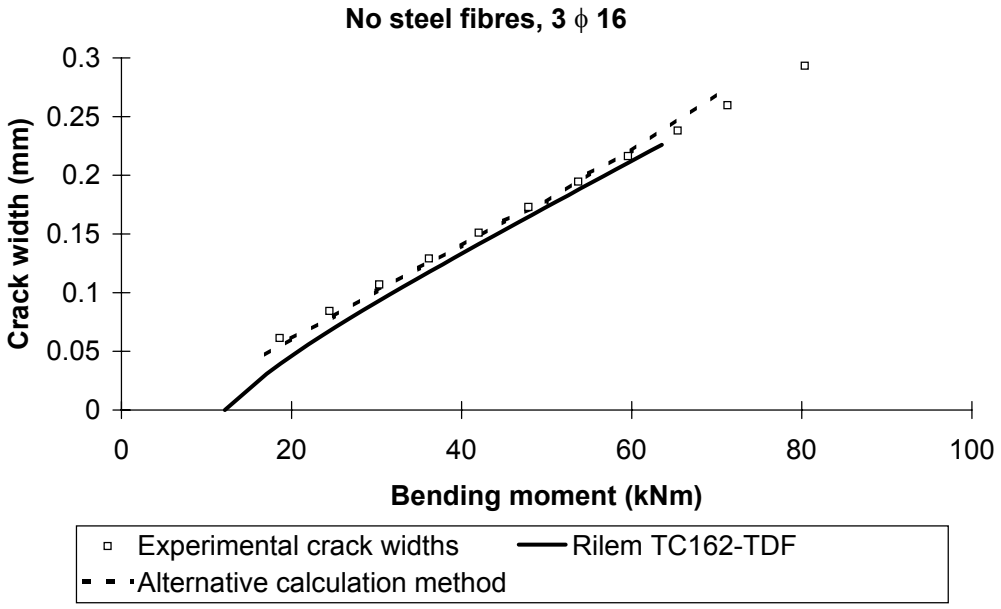

Figure 9: Experimental and theoretical crack widths for beam 5

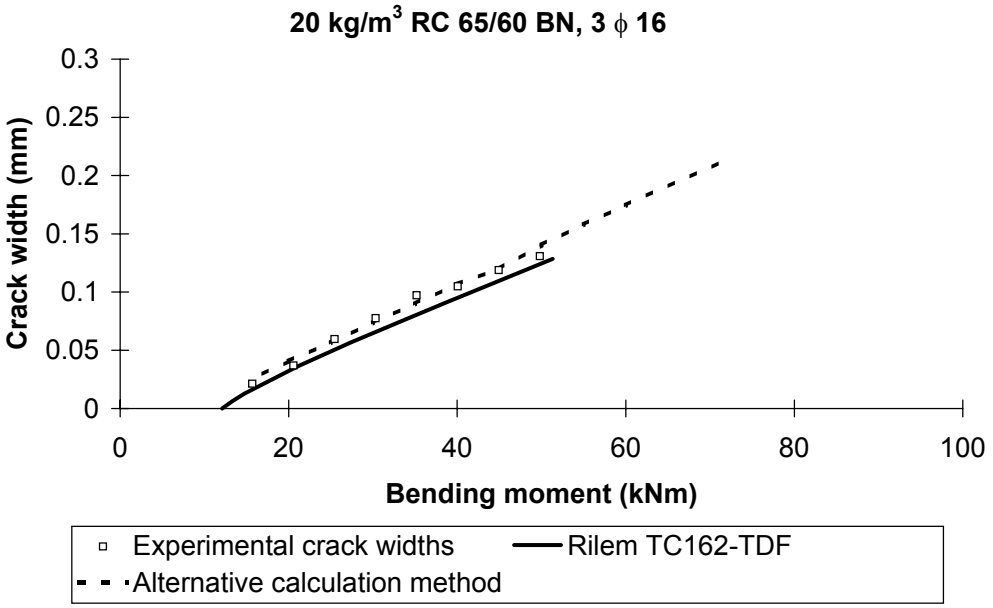

Figure 10: Experimental and theoretical crack widths for beam 6

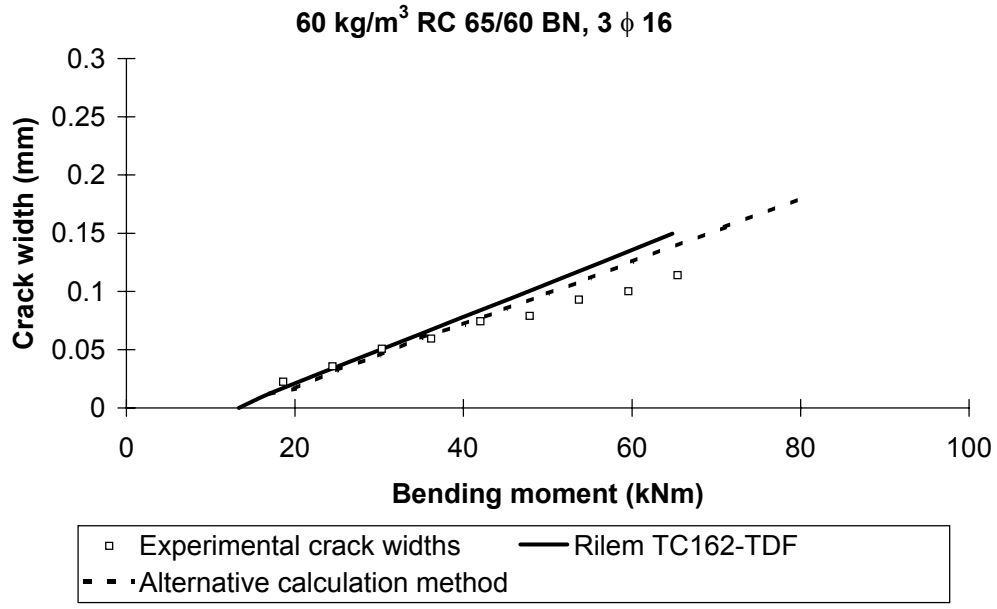

Figure 11: Experimental and theoretical crack widths for beam 7

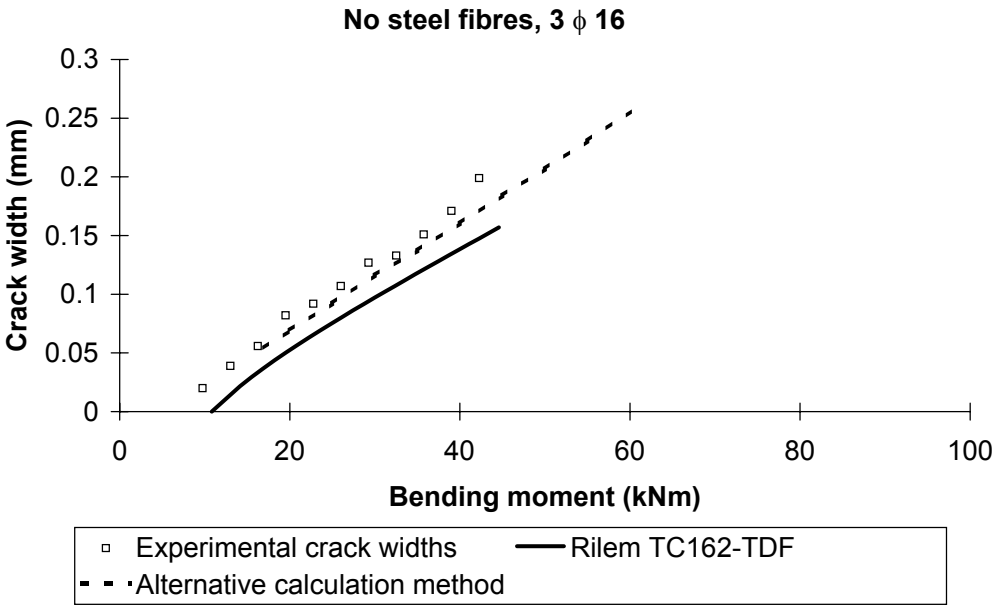

Figure 12: Experimental and theoretical crack widths for beam 8

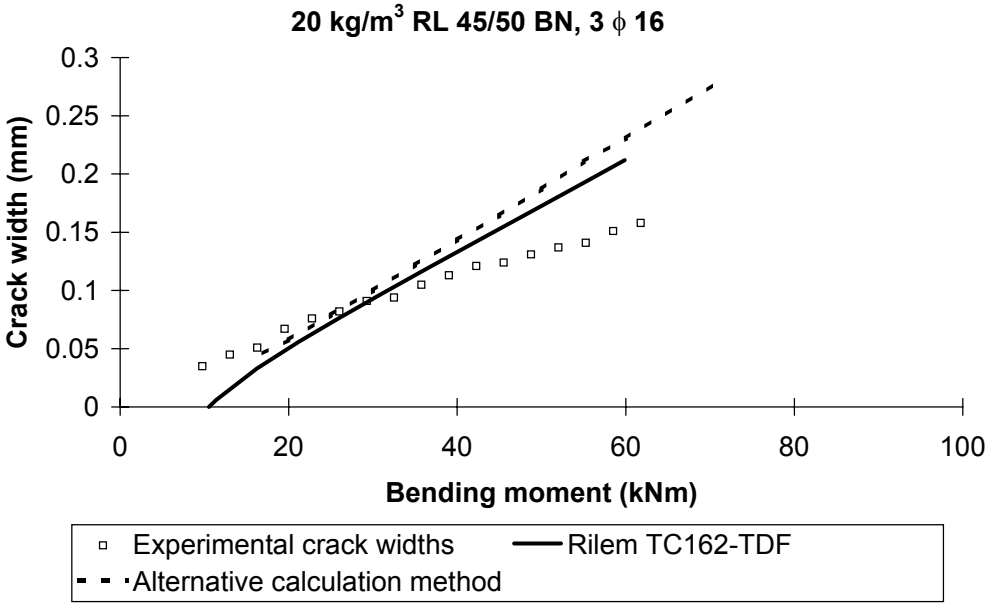

Figure 13: Experimental and theoretical crack widths for beam 9

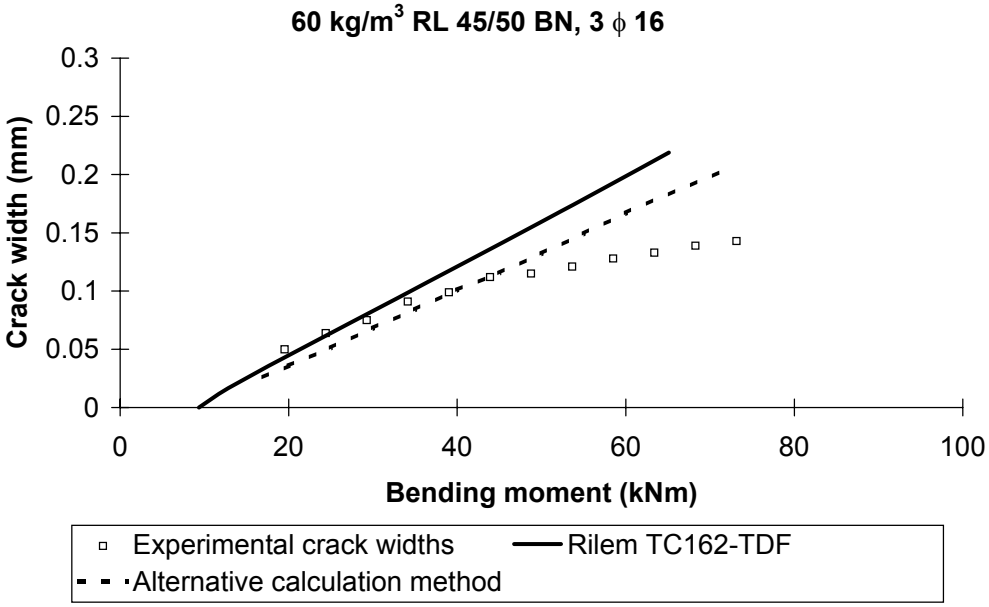

Figure 14: Experimental and theoretical crack widths for beam 10

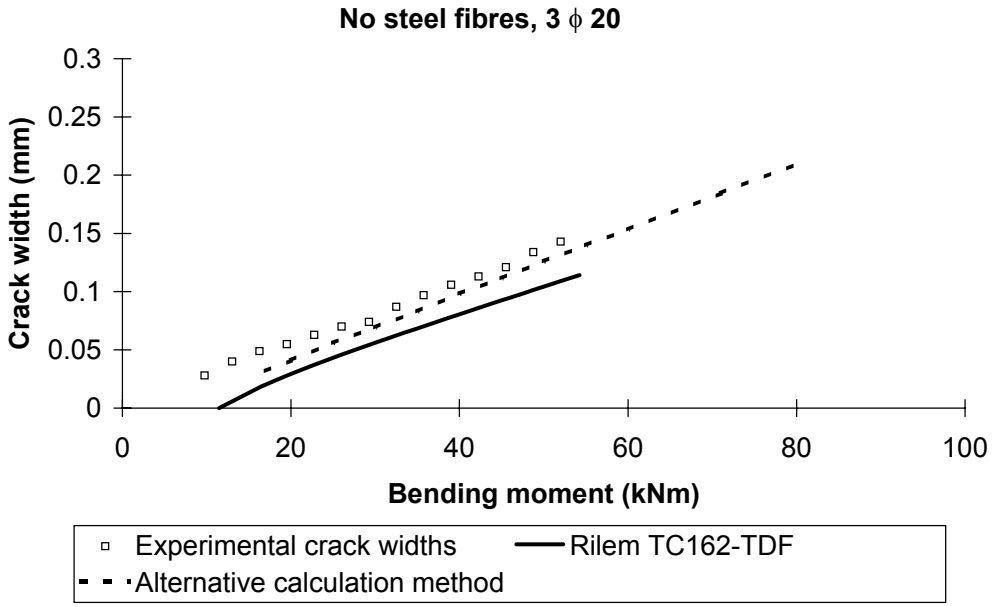

Figure 15: Experimental and theoretical crack widths for beam 11

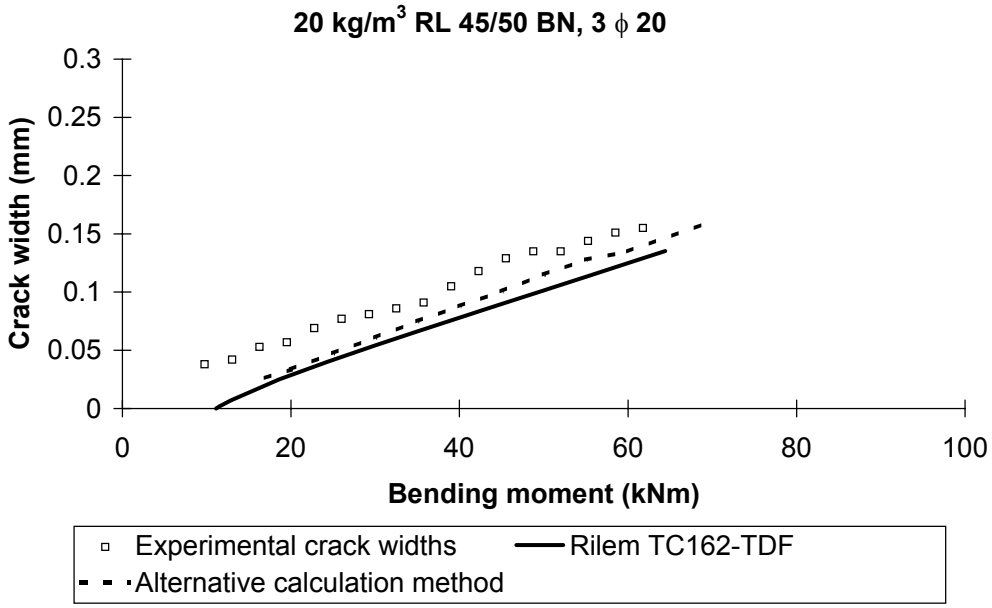

Figure 16: Experimental and theoretical crack widths for beam 12

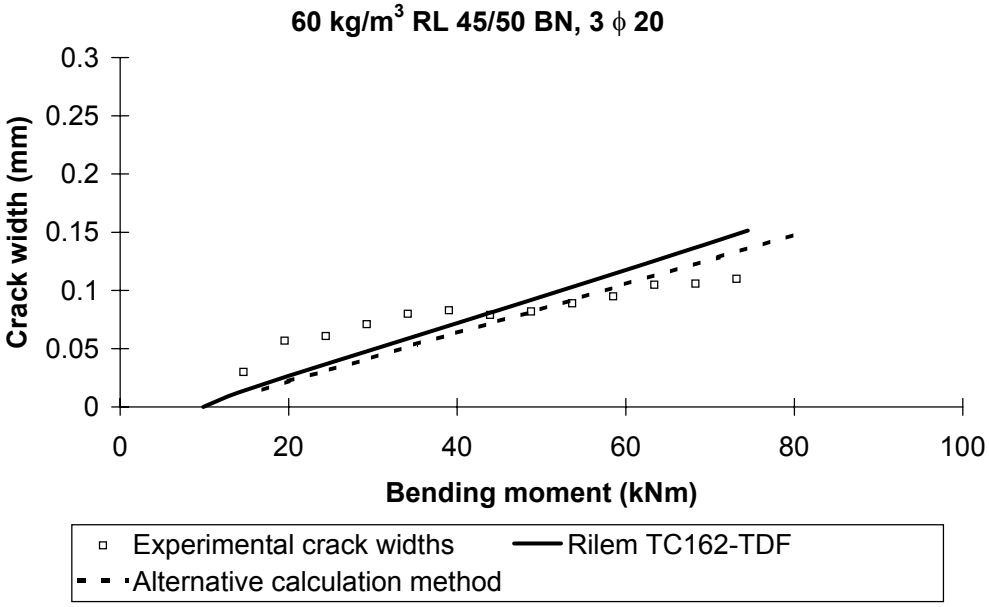

Figure 17: Experimental and theoretical crack widths for beam 13

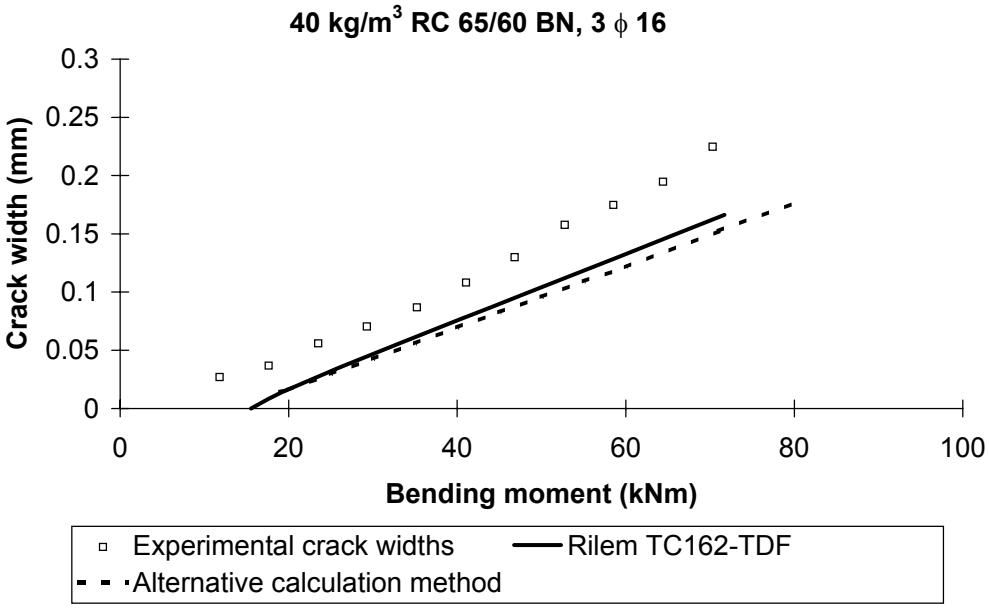

Figure 18: Experimental and theoretical crack widths for beam 14

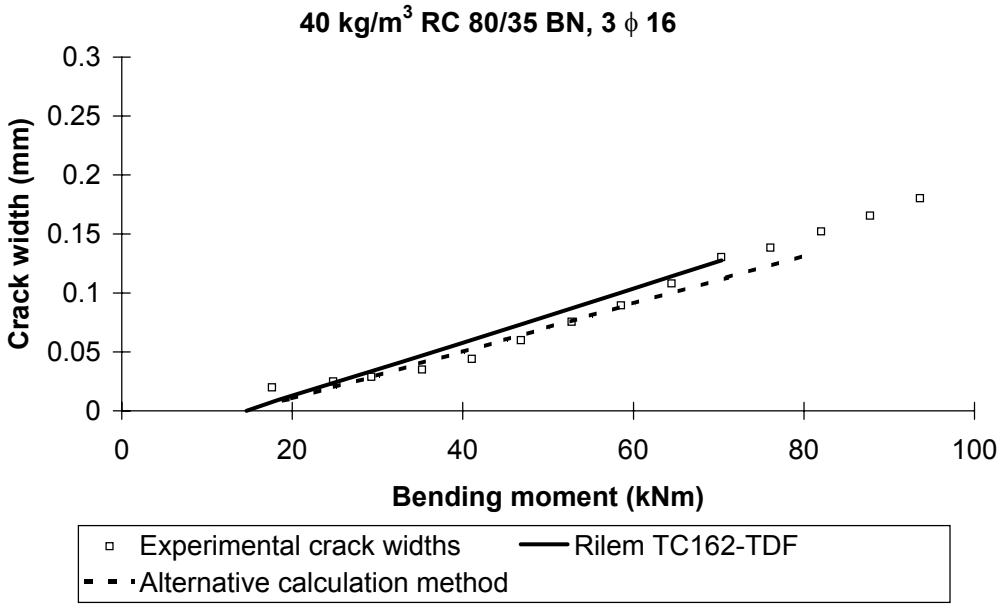

Figure 19: Experimental and theoretical crack widths for beam 15

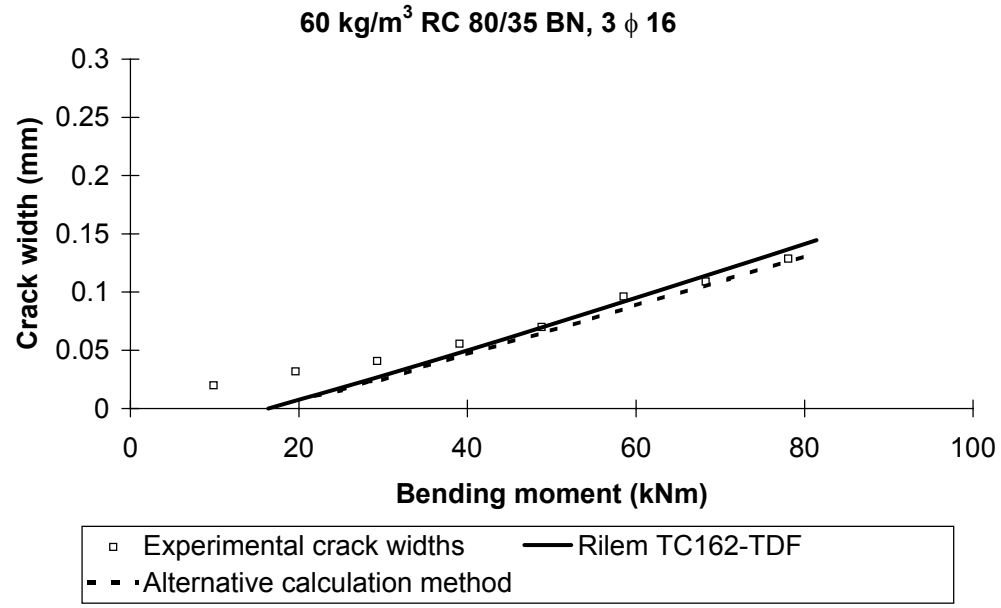

Figure 20: Experimental and theoretical crack widths for beam 16

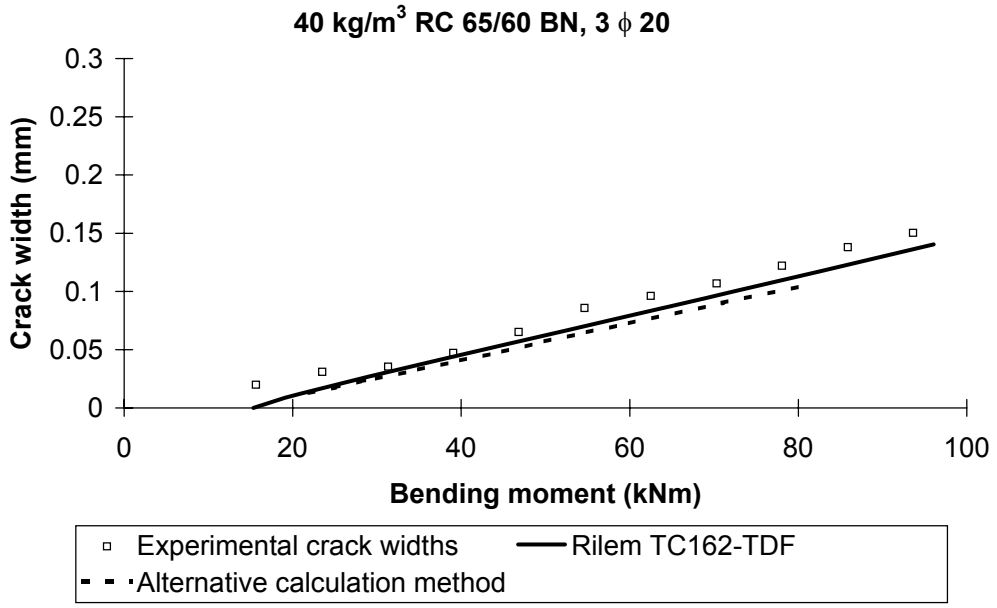

Figure 21: Experimental and theoretical crack widths for beam 17

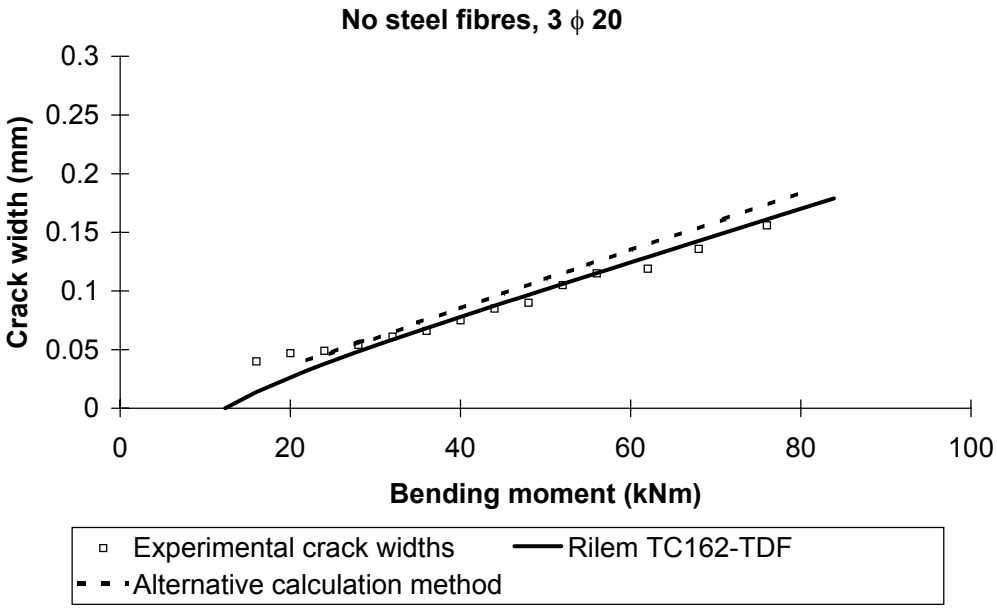

Figure 22: Experimental and theoretical crack widths for beam 18

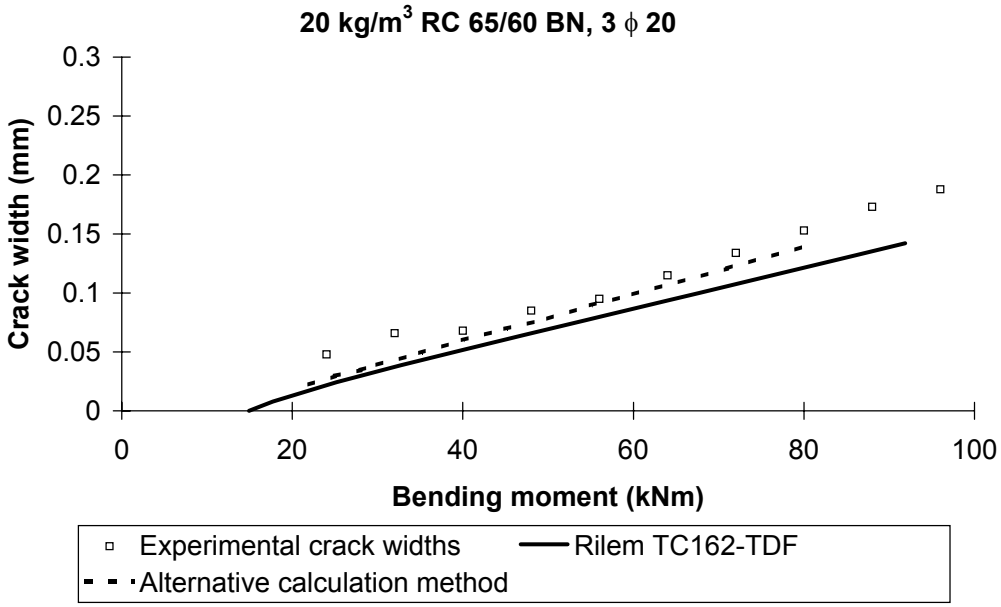

Figure 23: Experimental and theoretical crack widths for beam 19

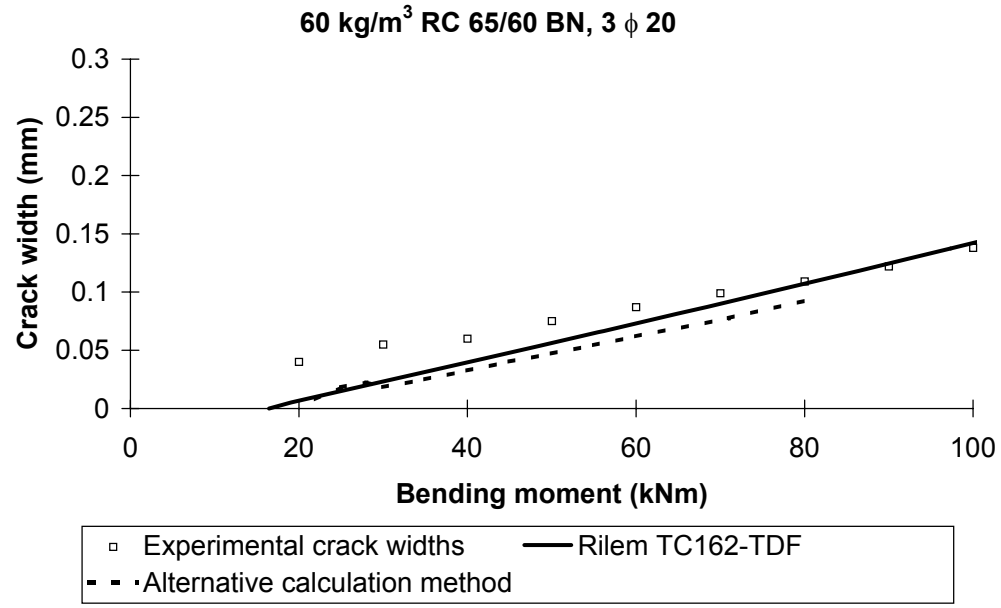

4. Conclusions

A large test program has been executed on 19 full-scale beams. The investigated parameters are the reinforcement ratio, the fibre dosage, the fibre type and the concrete strength. It can be

concluded from the test results that steel fibres have a strong beneficial effect on crack widths. For the same amount of longitudinal reinforcement, the addition of 60 kg/m^3 of steel fibres results clearly in a reduction of the crack widths. The benefit of the steel fibres is more obvious for the beams with 3 ϕ 16 than for the beams with 3 ϕ 20. This is logical since the portion of the fibres in the total tensile force of the beam is higher in this case.

Two calculation methods have been investigated. The first calculation method is a semi-empirical method, which is based on the calculation method of Eurocode 2. This first method is also the new proposal of the Rilem committee TC162-TDF. The second method is quite complicated and based on a physical model. The physical model takes into account the bond between the reinforcement bars and the surrounding concrete as well as the influence of the post-cracking tensile strength on the steel strain in a cracked section.

In comparing the calculated crack widths with the experimentally determined crack widths it becomes clear that, taking into account different assumptions as well as the uncertainty on the experimental results, the newly proposed alternative calculation method provides good predictions for all beams. Also the semi-empirical model provides accurate predictions of the crack widths. Since the semi-empirical method is much easier to use and the calculated crack widths are good predictions of the experimental crack widths, this method is by far the most suitable to be used as a standard method for crack width calculation. The newly proposed alternative calculation method on the other hand is rather complicated to use, but in return, it offers a very good insight in the mechanisms that determine the formation of cracks. With the alternative calculation method it becomes possible not only to calculate the crack width, but also the slip at any place between the reinforcement and the surrounding concrete as well as the course of the steel strain along the reinforcement.

5. Acknowledgements

This study was part of the Brite Euram project "Test and Design Methods for Steel Fibre Reinforced Concrete", contract n° BRPR-CT98-0813. The partners in the project are: N.V. Bekaert S.A. (Belgium, coordinator), Centre Scientifique et Technique de la Construction (Belgium), Katholieke Universiteit Leuven (Belgium), Technical University of Denmark (Denmark), Balfour Beatty Rail Ltd. (Great Britain), University of Wales Cardiff (Great Britain), Fertig-Decken-Union GmbH (Germany), Ruhr-University-Bochum (Germany), Technical University of Braunschweig (Germany), FCC Construcción S.A. (Spain), Universitat Polytècnica de Catalunya (Spain).

6. List of symbols

β_1	A coefficient which takes account of the bond properties of the bar	-
β_2	A coefficient which takes account of the duration of the load or of repeated loading	-
δ	Slip of the reinforcement bar relative to the surrounding concrete	mm
ΔF_s	Difference tensile force in the reinforcement between section 1 and section 2.	N
ε_c	Compression strain in the concrete	-
ε_{c1}	Compression strain in the concrete in section 1	-

ε_{c2}	Compression strain in the concrete in section 2	-
ε_{ct}	Tensile strain in the concrete at the moment of cracking	-
ε_s	Steel strain	-
ε_{s1}	Steel strain in section 1	-
ε_{s2}	Steel strain in section 2	-
ε_t	Tensile strain in the concrete	-
ε_{t1}	Tensile strain in the concrete in section 1	-
ε_{t2}	Tensile strain in the concrete in section 2	-
ε_{sm}	The mean steel strain	-
ϕ_b	Bar diameter	mm
ϕ_f	Fibre diameter	mm
λ	Bond parameter	1/mm
μ	Bond parameter	-
ρ_r	Effective reinforcement ratio	-
σ_c	The maximum stress in the concrete compression zone	N/mm^2
σ_s	The stress in the tensile reinforcement calculated on the basis of a cracked section	N/mm^2
σ_{sr}	The stress in the tensile reinforcement calculated on the basis of a cracked section under loading conditions causing first cracking	N/mm^2
τ	Bond stress between the reinforcement bar and the surrounding concrete	N/mm^2
A_s	Steel section	mm^2
$A_{c,eff}$	Effective tension area	mm^2
b	Width of the beam	mm
d	Effective depth of the beam	mm
h	Depth of the beam	mm
E_c	Youngs modulus for concrete	N/mm^2
E_s	Youngs modulus for steel	N/mm^2
f_{ctm}	Tensile strength of the concrete	N/mm^2
$f_{eq,2}$	Equivalent flexural tensile strength determined at a deflection of 0.65 mm	N/mm^2
$f_{eq,3}$	Equivalent flexural tensile strength determined at a deflection of 2.65 mm	N/mm^2
$f_{R,1}$	Residual flexural tensile strength determined at a CMOD of 0.5 mm	N/mm^2
$f_{R,4}$	Residual flexural tensile strength determined at a CMOD of 3.5 mm	N/mm^2
k_1	A coefficient which takes account of the bond properties of the bars	-
k_2	A coefficient which takes account of the form of the strain distribution	-
L	Maximum distance between a cracked section and a section that is just about to crack	mm
L_f	Fibre length	mm
M	Bending moment	kNm
s_{rm}	Average final crack spacing	mm

w_m	Average crack width	mm
x	Distance to a section that is just about to crack	mm
y	Height of the tensile zone	mm
z	Height of the compression zone	mm

7. References

[1] L. Vandewalle, Test and design methods of steel fibre reinforced concrete – Results of the Rilem Committee, Proceedings of the 2 Leipziger Fachtagung "Innovationen im Bauwesen": Faserbeton, 28-29 November 2002.

[2] ENV 1992-1-1: 1991, Eurocode 2 : Design of concrete structures - Part 1 : General rules and rules for buildings, 1991.

[3] D. Dupont and L. Vandewalle, Characterisation of steel fibre concrete with a σ–ε relation, Proceedings of the 4th international Ph.D. symposium in Civil Engineering, 19-21 September 2002, pp 108-114.

[4] L. Vandewalle, Hechting tussen wapening met verbeterde hechting en beton bij gewone en cryogene omstandigheden (in dutch), doctoral thesis, Catholic University of Leuven (Belgium), 1988.

[5] D. Dupont and L. Vandewalle, Influence of steel fibres in local bond behaviour, Proceedings of the international symposium "Bond in Concrete", Budapest, November 20-22, 2002.

[6] F. De Bonte, Hechtsterkte bij Staalvezelbeton (in dutch), Masters thesis, Catholic University of Leuven (Belgium), 2000.

[7] K. H. Tan, P. Paramasivam, K. C. Tan, Cracking Characteristics of Reinforced steel fibre concrete beams under short- and long-term loadings, Advanced cement based materials, Vol. 2, 1995, pp.127-137.

[8] L. Vandewalle et al. (2000): "Recommendations of Rilem TC162-TDF : Test and design methods for steel fibre reinforced concrete : bending test", Materials and Structures, 2000, Vol.33, pp.3-5.